


Simple and inexpensive technique for measuring oxygen consumption rate in adherent cultured cells

Eiji Takahashi¹  · Yoshihisa Yamaoka¹

Received: 10 May 2017 / Accepted: 25 July 2017 / Published online: 7 August 2017
© The Physiological Society of Japan and Springer Japan KK 2017

Abstract Measurement of cellular oxygen consumption rate (OCR) is essential in assessing roles of mitochondria in physiology and pathophysiology. Classical techniques, in which polarographic oxygen electrode measures the extracellular oxygen concentration in a closed measuring vessel, require isolation and suspension of the cell. Because cell functions depend on the extracellular milieu including the extracellular matrix, isolation of cultured cells prior to the measurement may significantly affect the OCR. More recent techniques utilize optical methods in which oxygen-dependent quenching of fluorophores determines oxygen concentration in the medium at a few microns above the surface of the cultured cells. These techniques allow the OCR measurement in cultured cells adhered to the culture dish. However, this technique requires special equipment such as a fluorescence lifetime microplate reader or specialized integrated system, which are usually quite expensive. Here, we introduce a simple and inexpensive technique for measuring OCR in adherent cultured cells that utilizes conventional fluorescence microscopy and a glassware called a gap cover glass.

Keywords Oxygen consumption · Mitochondria · Respiration · Oxygen measurement

Introduction

The mitochondrion produces energy (ATP) while playing an essential role in cell death, including necrosis and apoptosis. Thus, the organelle is central in life and death. Mammalian cells heavily depend on oxygen-supported ATP production in mitochondria called oxidative phosphorylation. Intracellular signals set up oxygen demand in mitochondria while oxygen availability in a cellular microenvironment defines actual oxygen consumption. Thus, measurement of cellular oxygen consumption rate (OCR) is essential in assessing roles of mitochondria in physiology and pathophysiology. Specifically, in addition to profiling the energy metabolism in specific cells or cell lines [1], OCR measurement allows monitoring cellular bioenergetic responses to altered energy demand and availability of energy substrates including oxygen. The information is served to elucidate the integrated cellular behaviors in hypoxia [2–4], metabolic reprogramming in cancer and other cells [3, 5, 6], the disease with compromised mitochondrial functions [7–9], and drug effects [10, 11]. In addition, OCR measurement is a useful tool for quality control of cells/tissues [12].

Currently available techniques for OCR measurement usually use a small amount of tissue, suspension of isolated cells or isolated mitochondria in a closed test vessel with appropriate medium, where the rate of decrease in oxygen concentration in the medium is measured to calculate OCR assuming negligible intracellular oxygen stores [13].

Measurement of dissolved oxygen in the suspension medium can be conducted by polarography using a Clark electrode (e.g., OXYGRAPH by Oroboros). Because cellular oxygen consumption produces diffusion gradients of oxygen concentration between the cell and the electrode, stirring of the suspension medium is required during the

✉ Eiji Takahashi
eiji@cc.saga-u.ac.jp

¹ Advanced Technology Fusion, Graduate School of Science and Engineering, Saga University, Saga 840-8502, Japan

measurement [14]. Because the physical dimensions of the test vessel equipped with polarography electrode are relatively large (a few ml), vigorous stirring is particularly important to ensure rapid equilibrations. In this, the rate of stirring should be carefully adjusted because vigorous stirring damages the cell. Furthermore, consumption of oxygen by the electrode potentially constitutes an artifact.

When utilizing this technique to adherent cultured cells, cells must be detached from the culture dish by trypsinization, dissociated, and suspended in the medium before the measurement. It is well known that cellular function and viability depend upon extracellular matrix. Therefore, detachment of the cell from the culture dish may significantly disturb the cellular homeostasis, leading in some cases to the cell death known as anoikis [15]. In addition, because the cell shape changes drastically immediately after trypsinization, this may also affect the OCR [16].

A more recent technique permits the measurement of adherent cells in culture dish in situ. Here, the electrochemical oxygen electrode is replaced with an optical technique using quenching of phosphorescence/fluorescence by oxygen (e.g., MitoXpress by Luxcel and Seahorse XF analyzers by Agilent Technologies) [17]. This technique has significantly reduced the sample volume for extracellular oxygen measurement to a few μl so that rapid equilibration in oxygen concentration between the cell and the extracellular medium above the cell monolayer may be attained. A commercial device, such as Seahorse, succeeded in fully integrating and automatizing the measurement processes in cells plated in a conventional multi-well dish, allowing a high-throughput OCR measurement. However, this sophisticated system is quite expensive.

Here, we introduce a simple and affordable technique for OCR measurement targeted for adherent cultured cells. This technique does not require trypsinization of the cell. It can be easily conducted in laboratories with small budgets where conventional fluorescence microscopy can be utilized.

Materials and methods

In the present technique, cells cultured on a glass cover slip are placed, with medium containing oxygen-sensitive dye, in a small closed volume ($<5 \mu\text{l}$) and the changes in oxygen dependent fluorescence intensity in the dye is followed to calculate OCR.

GCG (gap cover glass)

To produce a small closed volume in which oxygen measurement is conducted, we devised a glassware that we call the gap cover glass (GCG). We assembled two thin ($150 \mu\text{m}$) rectangular glass slips ($9 \times 18 \text{ mm}$) with a

$25 \times 18 \text{ mm}$ microscopy slide glass in such a way that the glass slips are placed in parallel with a 2-mm gap on the slide glass (Fig. 1a) [18].

Measurement procedures

In the present study, we used COS-7, Hep3B, and MDA-MB-231 cells to test the proposed OCR measurement. Cells were cultured to confluent on commercial glass slips for cell culture (Culture cover glass, Matsunami, $\phi 15 \text{ mm}$ for Hep3B cells; type I collagen coat cover glass, GG-12, Neuvitro, $\phi 12 \text{ mm}$ for COS-7 and MDA-MB-231 cells) using DMEM supplemented with 10% FCS and antibiotics. At the measurement, cells were washed twice with HEPES-Tyrode's solution containing 0.2 mM Tris(2,2'-bipyridyl) dichlororuthenium(II) hexahydrate (Ru-solution) as an optical oxygen probe [19]. After applying a small amount of silicone sealant (Corning) onto the surface of the GCG, cells on the cover glass were placed above the gap upside down (Fig. 1b) and the cover glass was lightly pressed against the GCG so that they attach firmly. Then, an aliquot of $\sim 8 \mu\text{l}$ HEPES-Tyrode's-Ru solution (indicated in dark grey in Fig. 1c) was slowly injected into the gap. Care was taken to avoid contamination of air bubbles in the HEPES-Tyrode's-Ru solution. Finally, the open ends of the gap were sealed with silicone sealant (Fig. 1d). Now the cells were confined in a small ($<5 \mu\text{l}$) closed volume. Ru-fluorescence intensity (excitation 425 nm, emission 605 nm) was measured every 1 or 2 min using a CCD camera (CoolSNAP MYO, Photometrics) attached to a conventional fluorescence microscope with a $4\times$ object lens (IX-71, Olympus). The measurement continued until the fluorescence level plateaued (Fig. 2a). When the fluorescence measurement was complete, the cell shape was checked and the cell number was counted in the phase-contrast images (Fig. 2). Here, one can visually confirm whether viability of the cell is still retained after the measurement. This is particularly important in experiments to examine the effect of drugs such as respiratory inhibitors.

Calibration

Changes in the Ru-fluorescence intensity were converted to those in oxygen concentration in the medium with an assumption of the Stern–Volmer relationship.

$$I_0/I = 1 + K_{sv}[\text{O}_2],$$

where I and I_0 represent the Ru-fluorescence intensity at an arbitrary oxygen concentration ($[\text{O}_2]$) and at $[\text{O}_2] = 0$, respectively, while K_{sv} is a constant. In practice, the equation was modified,

$$I_0/I_{21} \times I_{21}/I = 1 + K_{sv}[\text{O}_2]$$

$$[\text{O}_2] = (I_{21}/I \times k - 1)/K_{sv},$$

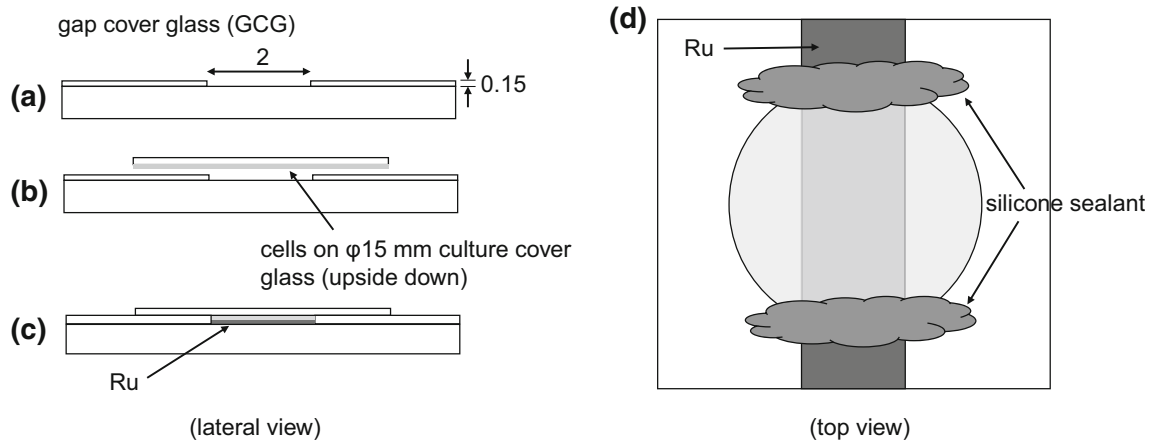


Fig. 1 Measurement of oxygen concentration in closed small extracellular volume. **a** Gap cover glass (GCG). **b** Cells cultured on a cover glass (indicated in *light grey*) is placed onto the gap (0.15 mm depth) in GCG in such a way that the cells face the gap. **c** HEPES-Tyrode's solution containing the Ru-compound (indicated in *dark grey*) is

slowly injected into the gap. **d** Finally, the open ends of the gap are sealed at the edge of the cover glass with silicone sealant. Changes in oxygen concentration in the thin medium layer above cells are followed by the Ru-fluorescence. Numbers in mm. Ru, HEPES-Tyrode's buffer containing the Ru-compound

where I_{21} represents Ru-fluorescence intensity at $[O_2] = 20.9\%$ (room air) and $k = I_0/I_{21}$ (constant). I_0 was defined as the Ru-fluorescence at the plateau (Fig. 2a). Because changes in the temperature immediately after placing the GCG on the temperature-controlled microscope stage affected the Ru-fluorescence, I_{21} was determined by linear extrapolation of the Ru-fluorescence in the rising phase (Fig. 2a). K_{sv} was calculated from I_0 and I_{21} . k and K_{sv} thus determined were 1.382 ± 0.046 (mean \pm SD, $n = 5$) and 0.0183 ± 0.0022 ($n = 5$), respectively.

Calculation of OCR

Using the linear rising phase of the Ru-fluorescence (dotted lines in Figs. 2a, 3), the rate of rise in the Ru-fluorescence was determined and subsequently converted to the rate of decrease in the oxygen concentration in %/min (A). Then, assuming the Henry's law constant for oxygen in water at $37\text{ }^\circ\text{C} = 1.41\text{ }\mu\text{mol/l/mmHg}$, the rate of decrease in oxygen concentration is converted to $\mu\text{mol/l/min}$,

$$A/100 \times 760 \times 1.41.$$

Finally, using separately determined cell number, N cells/ml, OCR in $\text{nmol/min}/10^6$ cells is calculated as follows:

$$A/100 \times 760 \times 1.41/N \times 10^6.$$

Results

Figure 2 illustrates representative OCR measurements in COS-7 cells. In untreated cells (Fig. 2a), following a small and transient dip in the Ru-fluorescence immediately after placing the GCG on the temperature-controlled ($37\text{ }^\circ\text{C}$)

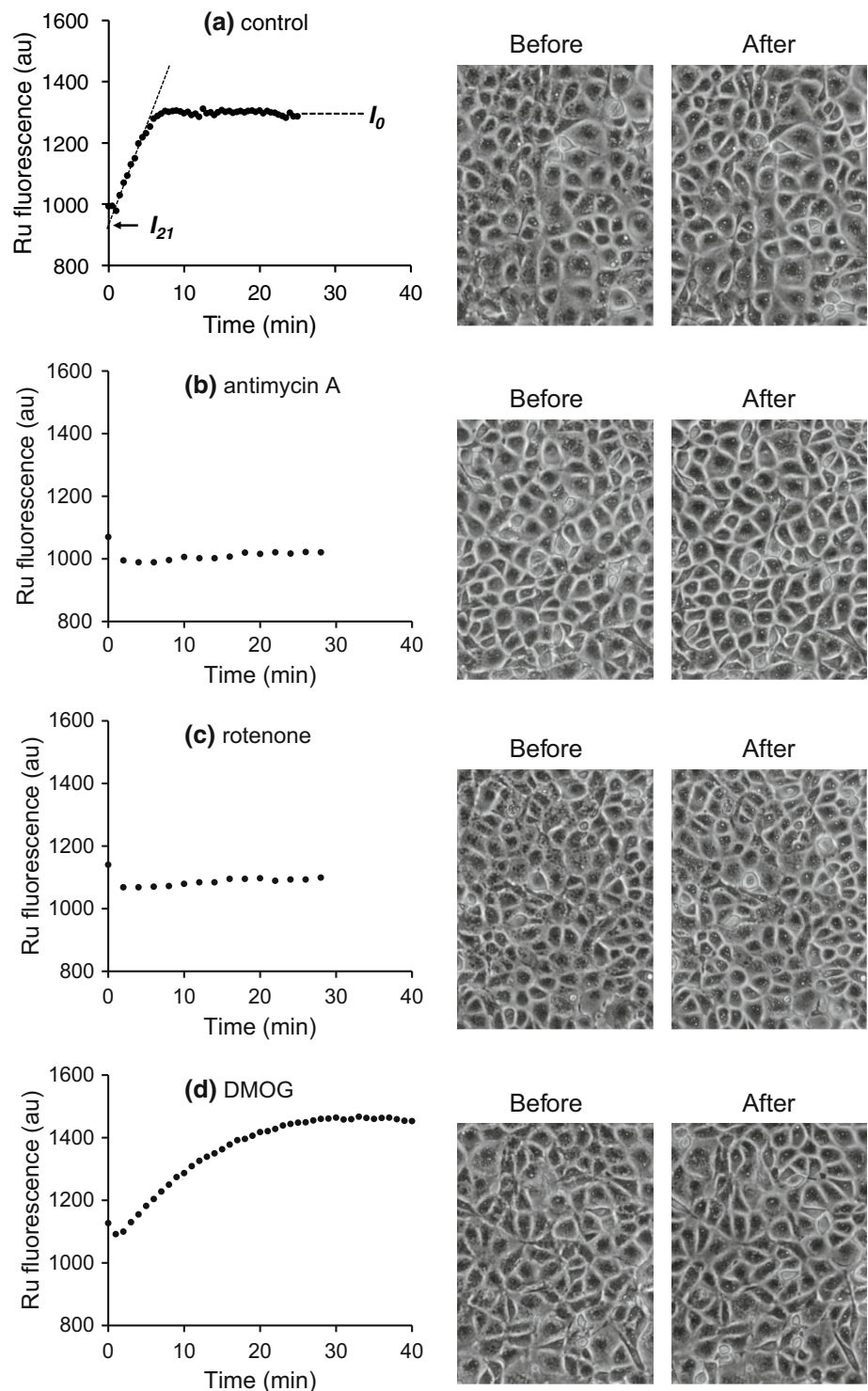
microscope stage, the Ru-fluorescence linearly increased, reflecting cellular consumption of oxygen in the closed volume. In untreated cells (Fig. 2a), the Ru-fluorescence reached the plateau within 10 min. We calculated I_{21} by extrapolation from the linear portion of the rising phase. Then, A was calculated using I_{21} and predetermined k and K_{sv} . When the fluorescence measurement was complete, the number of cells in the closed volume were counted in the phase-contrast images and converted to cells/ml. To determine the average cell number, we usually capture three images while changing the region of interest. The average OCR in COS-7 cells thus determined was $3.05 \pm 0.61\text{ nmol/min}/10^6$ cells ($n = 7$). Pharmacological inhibitions of the complex I and III in the respiratory chain by rotenone (Fig. 2c) and antimycin A (Fig. 2b), respectively, abolished OCR. Also, dimethylloxaloylglycine (DMOG) inductions of HIF-1 α (immunocytochemistry, data not shown) significantly suppressed mitochondrial respiration to $1.73 \pm 0.34\text{ nmol/min}/10^6$ cells ($n = 5$, Fig. 2d).

We also compared OCRs in cancer cell lines (Hep3B and MDA-MB-231) with non-cancer COS-7 cells (Fig. 3). Compared with COS-7 cells, OCRs were significantly lower both in Hep3B ($1.38 \pm 0.47\text{ nmol/min}/10^6$ cells, $n = 9$) and MDA-MB-231 ($1.09 \pm 0.29\text{ nmol/min}/10^6$ cells, $n = 6$) cells. DMOG treatment of Hep3B cells also significantly attenuated the OCR to $0.44 \pm 0.02\text{ nmol/min}/10^6$ cells ($n = 3$).

Discussion

One of the benefits of employing the proposed OCR measurements is that trypsinization is not required and OCR can be determined in cells as they grow in a culture

Fig. 2 Representative data demonstrating changes in the Ru-fluorescence in COS-7 cells with phase-contrast images of the cell before and after the measurement (300 $\mu\text{m} \times 400 \mu\text{m}$ rectangular area). Inhibition of the complex III and the complex I in the respiratory chain by antimycin A (10 μM) and rotenone (5 $\mu\text{g}/\text{ml}$), respectively, completely abolished the oxygen consumption (**b** and **c**, respectively). Treatment with 1 mM DMOG for 8 h significantly suppressed the oxygen consumption in COS-7 cells (**d**). Cell shapes did not change during the measurement



dish. The glassware (GCG) can be easily hand-made and conventional fluorescence microscope can be used. So, this technique costs substantially less than commercial systems and is particularly suitable for laboratories with a low budget. The time required for an OCR determination is usually less than 30 min in the present demonstrations,

evading the effect of the Ru-compound, if any, on cellular viability (see phase contrast images in Fig. 2). Furthermore, if the Ru-compound in the extracellular medium is replaced with a fluorescent indicator for pH, this technique would also allow measurement of the extracellular acidification rate similar to the Seahorse system.

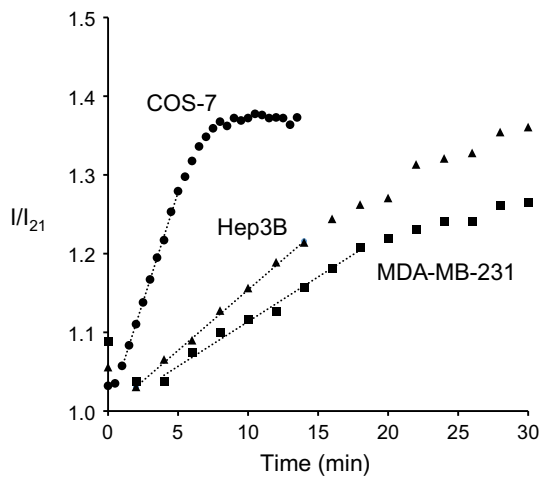


Fig. 3 Comparisons of changes in the normalized Ru-fluorescence between COS-7 (fibroblast-like cell line) and two cancer cell lines, Hep3B and MDA-MB-231. *Dotted lines* indicate the slope of the Ru-fluorescence changes that is used for OCR calculations. OCRs in these cells were $3.85 \text{ nmol/min}/10^6$ cells in COS-7 cells, $1.48 \text{ nmol/min}/10^6$ cells in Hep3B cells, and $0.89 \text{ nmol/min}/10^6$ cells in MDA-MB-231 cells

For the conversion of Ru-fluorescence intensity to oxygen concentration, we used I_{21} , the Ru-fluorescence intensity at 20.9% oxygen (room air) rather than I_0 , Ru-fluorescence intensity at 0% oxygen. This arises from considerations that prolonged time is needed for the Ru-fluorescence to reach the plateau (0% oxygen) in experiments with partial respiratory inhibitions (see Fig. 2d for example). For the I_{21} at 37 °C, linear extrapolation in the rising phase of the Ru-fluorescence was conducted since Ru-fluorescence temporarily decreases at the transition from room temperature to 37 °C (Fig. 2a).

In the present study, oxygen-dependent quenching of the Ru-compound was utilized to assess the oxygen concentration in the extracellular medium. We selected the compound because the fluorescence wavelength (605 nm) does not overlap that of the major endogenous fluorophores such as NADH and FAD (fluorescence peaks at ~ 460 and ~ 520 nm, respectively) that may change according to the oxygen availability. Effects of the cellular autofluorescence were examined in COS-7 cells where the autofluorescence was measured without the Ru-compound in the medium. The fluorescence certainly increased in the aerobic to anaerobic transition but the magnitude was $<0.7\%$ of the Ru-fluorescence. This fluorescence change corresponds to a change in oxygen concentration for $<0.4\%$ and constitutes a $\sim 2\%$ offset in the present OCR measurement.

Intrinsic OCR value of a cell may vary according to the culture/measurement conditions. In addition, oxygen concentration changes in the extracellular bulk medium measured by conventional techniques should be standardized

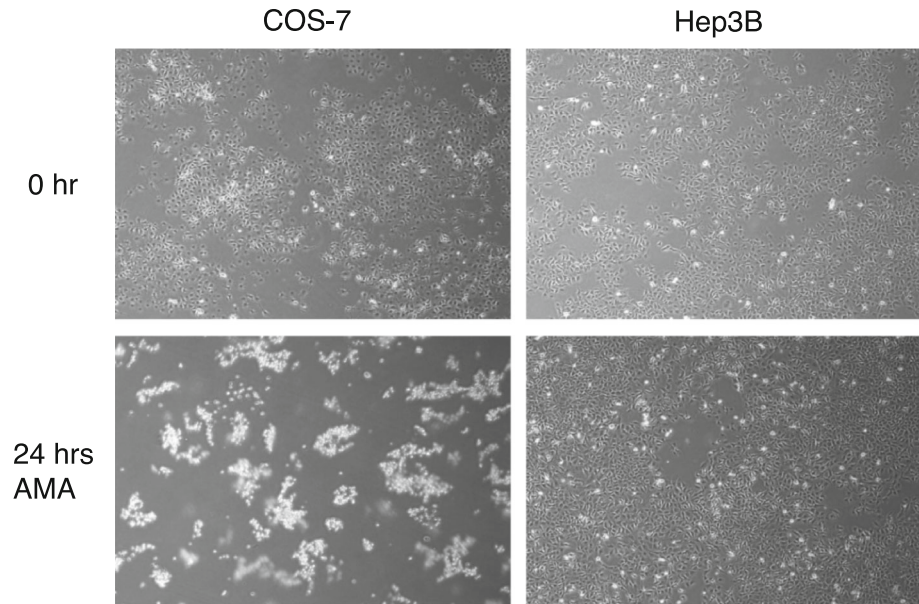
before assessing OCR per cell (also see Ref. [20] for single-cell OCR measurement). These facts indicate that there is no golden number for the OCR value for a specific cell. With these limitations in mind, we here compare the present OCR values with the reported ones.

Although published data for OCR in specific cell lines are generally scarce [21], the present OCR value for Hep3B cells may be compared with that reported by Metzen et al. [22]. They conducted an OCR measurement in monolayers of cultured Hep3B cells. By firmly pressing the specially designed steel attachment with a “cage” in which stirring bar was housed to the culture dish filled with culture medium, they performed OCR measurements with conventional polarographic oxygen electrode, without detaching the cell from the bottom of the culture dish. They reported that OCR in Hep3B cells was $9.6 \pm 1.4 \text{ nmol/min/mg protein}$. With the value $0.13 \text{ mg protein/cm}^2$ in confluent monolayer Hep3B cells reported in the same paper, the reported OCR value can be converted to $1.1 \text{ nmol/min}/10^6$ cells, which is quite close to the present result. Recently, single-cell OCR measurement was reported in MDA-MB-231 cells [20]. Although the OCR value for individual cells was highly variable, the median for the single-cell OCR values in these cells was 0.80 fmol/min , which is close to the value in the present study ($1.09 \text{ nmol/min}/10^6$ cells).

The OCR in Hep3B cells was significantly lower than COS-7 cells (Fig. 3). Because cellular OCR depends on various factors including cell size, mitochondria mass, respiratory enzyme activities, oxygen concentration at mitochondria, mitochondrial respiratory control, uncoupling proteins, and non-mitochondrial oxygen consumptions, simple comparisons of OCRs among different cell lines are obviously inappropriate. However, the prolonged survival of Hep3B cells without oxidative phosphorylation (i.e., inhibition of the complex III in the respiratory chain by antimycin A, see Fig. 4) compared to COS-7 cells, together with the OCR data mentioned above, may imply a less dependency of Hep3B cells (a cancer cell line) on oxidative phosphorylation compared to COS-7 cells (a fibroblast-like cell line). Thus, profiling of cellular energy metabolism is possible from the present OCR measurement. The difference in the OCR in these cell lines appears to be consistent with the Warburg effect in cancer cells in vivo where ATP production by anaerobic glycolysis is significantly enhanced even in the presence of ample oxygen [23].

Similar to the Warburg effect in cancer cells, hypoxic induction of HIF-1 α leads to enhanced glycolysis while significantly suppressing oxidative phosphorylation through multiple mechanisms [3, 24]. The response named metabolic reprogramming appears to be an ingenious way for cells not only to adapt oxygen depletions but also to prevent production of excess ROS in mitochondria [24]. Dimethylxaloylglycine, a competitive blocker of proryl

Fig. 4 Phase-contrast images of COS-7 (a fibroblast-like cell line) and Hep3B (a cancer cell line) cells after 24-h treatment with antimycin A (AMA, 10 μ M). Absence of oxidative ATP production for 24 h almost completely killed COS-7 cells (i.e., detached from the dish bottom and shrunken), while Hep3B cells appeared viable (the number of the intact cell was 95% of the untreated control). With the OCR data indicated in Fig. 3, a metabolic profiling of these distinct cell lines may be possible



hydroxylase, mimics hypoxic induction of the HIF-1 α pathway [25] in normoxic cells. DMOG has been demonstrated to significantly reduce mitochondrial respiration [26] similar to metabolic reprogramming in hypoxia. Present OCR measurement successfully demonstrated considerable reductions of OCR after \sim 8 h treatment with DMOG in COS-7 and Hep3B cells while the OCR was not affected by acute (1 h) DMOG administrations.

In summary, we have developed a simple and inexpensive technique for measuring OCR in adherent cultured cells. Using this technique, we have determined the OCR in COS-7, Hep3B, and MDA-MB-231 cells. The OCR in Hep3B and MDA-MB-231 cells is comparable with the previous reports. With the present OCR measurements, we demonstrated a cancer cell line profiling and DMOG-induced respiratory suppressions.

Compliance with ethical standards

Conflict of interest The authors declare no conflicts of interest.

Funding Part of this work was supported by JSPS KAKENHI Grant Number 26430117.

Ethical approval This article does not contain any studies with human participants or animals performed by any of the authors.

References

- Kramer PA, Ravi S, Chacko B, Johnson MS, Darley-USmar VM (2014) A review of the mitochondrial and glycolytic metabolism in human platelets and leukocytes: implications for their use as bioenergetic biomarkers. *Redox Biol* 2:206–210
- Hagen T, Taylor CT, Lam F, Moncada S (2003) Redistribution of intracellular oxygen in hypoxia by nitric oxide: effect on HIF1 α . *Science* 302:1975–1978
- Papandreou I, Cairns RA, Fontana L, Lim AL, Denko NC (2006) HIF-1 mediates adaptation to hypoxia by actively downregulating mitochondrial oxygen consumption. *Cell Metab* 3:187–197
- Scandurra FM, Gnaiger E (2010) Cell respiration under hypoxia: facts and artefacts in mitochondrial oxygen kinetics. *Adv Exp Med Biol* 662:7–25
- Agostini M, Romeo F, Inoue S, Niklison-Chirou MV, Elia AJ, Dinsdale D, Morone N, Knight RA, Mak TW, Melino G (2016) Metabolic reprogramming during neuronal differentiation. *Cell Death Differ* 23:1502–1514
- Semenza GL (2007) Oxygen-dependent regulation of mitochondrial respiration by hypoxia-inducible factor 1. *Biochem J* 405:1–9
- Horan MP, Pichaud N, Ballard JW (2012) Review: quantifying mitochondrial dysfunction in complex diseases of aging. *J Gerontol A Biol Sci Med Sci* 67:1022–1035
- Lestienne P (1999) Mitochondrial diseases. Models and methods. Springer, Berlin
- Schuh RA, Jackson KC, Schlappal AE, Spangenburg EE, Ward CW, Park JH, Dugger N, Shi GL, Fishman PS (2014) Mitochondrial oxygen consumption deficits in skeletal muscle isolated from an Alzheimer's disease-relevant murine model. *BMC Neurosci* 15:24
- Schulze-Osthoff K, Bakker AC, Vanhaesebroeck B, Beyaert R, Jacob WA, Fiers W (1992) Cytotoxic activity of tumor necrosis factor is mediated by early damage of mitochondrial functions. Evidence for the involvement of mitochondrial radical generation. *J Biol Chem* 267:5317–5323
- Souid AK, Tacka KA, Galvan KA, Penefsky HS (2003) Immediate effects of anticancer drugs on mitochondrial oxygen consumption. *Biochem Pharmacol* 66:977–987
- Sweet IR, Gilbert M, Scott S, Todorov I, Jensen R, Nair I, Al-Abdullah I, Rawson J, Kandeel F, Ferreri K (2008) Glucose-stimulated increment in oxygen consumption rate as a standardized test of human islet quality. *Am J Transplant* 8:183–192
- Simonnet H, Vigneron A, Pouyssegur J (2014) Conventional techniques to monitor mitochondrial oxygen consumption. *Methods Enzymol* 542:151–161
- Papas KK, Pisanía A, Wu H, Weir GC, Colton CK (2007) A stirred microchamber for oxygen consumption rate measurements with pancreatic islets. *Biotechnol Bioeng* 98:1071–1082

15. Frisch SM, Screaton RA (2001) Anoikis mechanisms. *Curr Opin Cell Biol* 13:555–562
16. Danhier P, Copetti T, De Preter G, Leveque P, Feron O, Jordan BF, Sonveaux P, Gallez B (2013) Influence of cell detachment on the respiration rate of tumor and endothelial cells. *PLoS One* 8:e53324
17. Papkovsky DB, Zhdanov AV (2016) Phosphorescence based O₂ sensors—essential tools for monitoring cell and tissue oxygenation and its impact on metabolism. *Free Radic Biol Med* 101:202–210
18. Yahara D, Yoshida T, Enokida Y, Takahashi E (2016) Directional migration of MDA-MB-231 cells under oxygen concentration gradients. *Adv Exp Med Biol* 923:129–134
19. Dobrucki JW (2001) Interaction of oxygen-sensitive luminescent probes Ru(phen)₃²⁺ and Ru(bipy)₃²⁺ with animal and plant cells in vitro. Mechanism of phototoxicity and conditions for non-invasive oxygen measurements. *J Photochem Photobiol B* 65:136–144
20. Kelbauskas L, Glenn H, Anderson C, Messner J, Lee KB, Song G, Houkal J, Su F, Zhang L, Tian Y, Wang H, Bussey K, Johnson RH, Meldrum DR (2017) A platform for high-throughput bioenergy production phenotype characterization in single cells. *Sci Rep* 7:45399. doi:10.1038/srep45399
21. Wagner BA, Venkataraman S, Buettner GR (2011) The rate of oxygen utilization by cells. *Free Radic Biol Med* 51:700–712
22. Metzén E, Wolff M, Fandrey J, Jelkmann W (1995) Pericellular PO₂ and O₂ consumption in monolayer cell cultures. *Respir Physiol* 100:101–106
23. Koppenol WH, Bounds PL, Dang CV (2011) Otto Warburg's contributions to current concepts of cancer metabolism. *Nat Rev Cancer* 11:325–337
24. Semenza GL (2012) Hypoxia-inducible factors in physiology and medicine. *Cell* 148:399–408
25. Elvidge GP, Glenny L, Appelhoff RJ, Ratcliffe PJ, Ragoussis J, Gleadle JM (2006) Concordant regulation of gene expression by hypoxia and 2-oxoglutarate-dependent dioxygenase inhibition: the role of HIF-1 α , HIF-2 α , and other pathways. *J Biol Chem* 281:15215–15226
26. Zhdanov AV, Okkelman IA, Collins FW, Melgar S, Papkovsky DB (2015) A novel effect of DMOG on cell metabolism: direct inhibition of mitochondrial function precedes HIF target gene expression. *Biochim Biophys Acta* 1847:1254–1266